No evidence for bulk velocity from type Ia supernovae

Journal of Cosmology and Astroparticle Physics
An IOP and SISSA journal

No evidence for bulk velocity from type Ia supernovae

Dragan Huterer,[a,b,c] **Daniel L. Shafer**[a] **and Fabian Schmidt**[b]

[a]Department of Physics, University of Michigan,
450 Church Street, Ann Arbor, MI 48109, U.S.A.
[b]Max-Planck-Institut für Astrophysik,
Karl-Schwarzschild-Str. 1, 85748 Garching, Germany
[c]Excellence Cluster Universe,
Boltzmannstr. 2, D-85748 Garching, Germany

E-mail: huterer@umich.edu, dlshafer@umich.edu, fabians@mpa-garching.mpg.de

Received October 1, 2015
Revised November 25, 2015
Accepted December 2, 2015
Published December 16, 2015

Abstract. We revisit the effect of peculiar velocities on low-redshift type Ia supernovae. Velocities introduce an additional guaranteed source of correlations between supernova magnitudes that should be considered in all analyses of nearby supernova samples but has largely been neglected in the past. Applying a likelihood analysis to the latest compilation of nearby supernovae, we find no evidence for the presence of these correlations, although, given the significant noise, the data is also consistent with the correlations predicted for the standard ΛCDM model. We then consider the dipolar component of the velocity correlations — the frequently studied "bulk velocity" — and explicitly demonstrate that including the velocity correlations in the data covariance matrix is crucial for drawing correct and unambiguous conclusions about the bulk flow. In particular, current supernova data is consistent with no excess bulk flow on top of what is expected in ΛCDM and effectively captured by the covariance. We further clarify the nature of the apparent bulk flow that is inferred when the velocity covariance is ignored. We show that a significant fraction of this quantity is expected to be noise bias due to uncertainties in supernova magnitudes and not any physical peculiar motion.

Keywords: supernova type Ia - standard candles, cosmic flows

ArXiv ePrint: 1509.04708

doi:10.1088/1475-7516/2015/12/033

Contents

1 Introduction

Motions of objects in the universe are not entirely random. Objects which are physically close to one another respond similarly to the pull of large-scale structure, and as a result their peculiar velocities are correlated. Correlations between galaxy peculiar velocities are an old subject [1–7], and these velocities have already been used to constrain cosmological models, in particular the amount of matter in the universe (see [8] for a review). More recently, peculiar velocities have become important in the analysis of type Ia supernova (SN Ia) data. At low redshift ($z \lesssim 0.05$), typical peculiar velocities of $\sim 300\,\mathrm{km/s}$ are a significant contribution to the SN redshift (for instance, $cz = 3,000\,\mathrm{km/s}$ at $z = 0.01$). These peculiar velocities are a nuisance if one is interested in using the SNe to constrain expansion history and dark energy, and it is common practice to propagate this extra dispersion into the error budget (e.g. add $300\,\mathrm{km/s} \times 5/(cz \ln 10)$ in quadrature to the statistical uncertainty of each SN magnitude). However, this neglects significant covariance between the velocities of different SNe.

Alternatively, one can consider the SN peculiar velocity field itself to be a signal, one that should contain useful information about the amount and distribution of matter in the universe. Nearby SNe are much fewer in number than nearby galaxies, and given the volume limitation for both, this will likely still be the case in the future. On the other hand, SNe are more useful on a per-object basis because their individual distances can be inferred directly and with relative precision — roughly 7% for each SN, depending on the quality of the observations. Therefore, there has been a resurgence of interest in how SN peculiar velocities are modeled and used [9, 10].

In this paper, we perform a careful study of the SN velocity correlations in current data, in particular the way in which they are used to draw conclusions about the so-called "bulk velocity" — the motion, relative to the cosmic microwave background (CMB) rest frame, of the patch of the universe centered on us and containing the nearby sample. Though we focus on SNe, our methodology is not restricted to SNe and equally applies to analysis of galaxy peculiar velocities.

The paper is organized as follows. In section 2, we review the physics of how peculiar velocities affect SN magnitudes. In section 3, we describe the SN samples and how we use them. In section 4, we define a general likelihood that is the basis for our analyses, which include a test for the presence of velocity correlations (section 5), a test for the presence of excess bulk velocity beyond that encoded in the correlations predicted in ΛCDM (section 6), and a comparison to previous work that studied bulk flows without the velocity covariance (section 7). We summarize our conclusions in section 8.

2 Theoretical framework

2.1 Magnification and SN magnitude residuals at low redshifts

The magnitude residuals of standard candles like SNe Ia are directly related to the magnification μ, which is defined as the fractional perturbation in the angular diameter and luminosity distances (see [9, 11]),

$$-\frac{1}{2}\,\mu = \frac{\Delta d_L}{\bar{d}_L(z)} = \frac{\Delta d_A}{\bar{d}_A(z)}\,, \tag{2.1}$$

where $\bar{d}_A(z)$ and $\bar{d}_L(z)$ denote the background distances evaluated at the observed redshift z. The second equality, relating luminosity and angular diameter distances, follows from the conservation of the photon phase space density. That is, μ describes both the change in the apparent angular size of a spatial ruler as well as the change in observed flux of a standard candle.

Covariant expressions for the magnification at linear order in cosmological perturbations have been given in [11–14]. In the conformal-Newtonian (cN) gauge, where the metric is written as

$$ds^2 = a^2(\tau)\big[-(1+2\Psi)\,d\tau^2 + (1+2\Phi)\,\delta_{ij}\,dx^i dx^j\big]\,, \tag{2.2}$$

the magnification is given, in the notation of [14], by[1]

$$\mu = \left[-2 + \frac{2}{aH\tilde{\chi}}\right]\Delta\ln a - 2\Phi + 2\kappa - 2v_{\parallel o} - \frac{2}{\tilde{\chi}}\int_0^{\tilde{\chi}} d\chi\,(\Psi - \Phi)\,, \tag{2.3}$$

where $\tilde{\chi} \equiv \chi(z)$ is the coordinate distance inferred using the observed redshift, and

$$\kappa = \frac{1}{2}\int_0^{\tilde{\chi}} d\chi\,\frac{\chi}{\tilde{\chi}}(\tilde{\chi} - \chi)\nabla_\perp^2(\Psi - \Phi)\,, \tag{2.4}$$

$$\Delta\ln a = \Psi_o - \Psi + v_\parallel - v_{\parallel o} + \int_0^{\tilde{\chi}} d\chi\big[\Phi' - \Psi'\big] \tag{2.5}$$

are the convergence and fractional redshift perturbation, respectively. The latter contains the gravitational redshift, Doppler shift, and integrated Sachs-Wolfe effect. Further, $\nabla_\perp^2$ denotes the Laplacian on a sphere of radius χ, $v_\parallel = v^i\hat{n}_i$ denotes the peculiar velocity projected along the line of sight $\hat{\mathbf{n}}$, integrals over χ denote integrals along the past lightcone, and a

[1] Here, we have neglected a term that is present if the luminosity of the standard candle depends on time; in any case, it is subdominant in the limit we will consider. We have also neglected two pure monopole contributions, motivated by the discussion in section 2.2.

JCAP12(2015)033

subscript o denotes a quantity evaluated at the location of the observer. Note that κ, $\Delta \ln a$, and any other terms appearing in eq. (2.3) are coordinate-dependent quantities, and only the combination given in eq. (2.3) corresponds to an actual (gauge-invariant) observable. This can be verified by considering gauge transformations and various test cases [14, 15].

For low-redshift SNe, where $z \ll 1$ so that $\tilde{\chi} \ll 1/(aH)$, the terms involving the velocity are the most significant. This is because the lensing convergence is suppressed for small source distances and because the scales probed are much smaller than the horizon. Then, the terms involving the potentials Φ and Ψ are also suppressed by roughly $aH\tilde{\chi}$ relative to the velocity. In this case, we obtain

$$\mu \overset{z \ll 1}{=} \frac{2}{aH\tilde{\chi}}(v_\parallel - v_{\parallel o})\,. \tag{2.6}$$

This expression for the magnification, proportional to the relative velocity along the line of sight between source and observer, simply arises due to the fact that we evaluate the luminosity distance to a supernova using the background distance-redshift relation, while the actual redshift is perturbed by the Doppler shift. One can easily verify numerically that this approximation is better than 1% for $z \lesssim 0.1$, which is the redshift range we will consider in this paper. Note that [9] includes the term -2 in the $\Delta \ln a$ prefactor in eq. (2.3); however, this is not strictly consistent, since the terms involving Ψ in $\Delta \ln a$, as well as the aberration term $-2v_{\parallel o}$ in eq. (2.3) are of comparable magnitude to this correction (see also [16]). We will thus work with eq. (2.6) as the proper low-z limit of eq. (2.3). Note that this relation remains valid even if μ becomes of order unity, as long as the velocities $v_\parallel$ remain small compared to the speed of light. On very small scales ($z < 0.01$), the velocities are no longer described accurately by linear perturbation theory. However, since the SN samples considered here are restricted to $z \gtrsim 0.01$, we will work with velocities derived from linear perturbation theory. Note that, in principle, nonlinear corrections to the velocity could also be relevant for higher-redshift SNe, if two SNe happen to be physically close. However, we have verified that nonlinear corrections to the velocities have a small effect (see below).

As eq. (2.6) shows, the relevant quantity for the magnification at low z is the relative velocity between the source and the observer projected along the line of sight. This also includes small-scale motions such as the velocity of the Solar System with respect to the Milky Way center, which are uncorrelated with large-scale cosmological velocity fields. For this reason, we correct the observed SN redshifts to the CMB rest frame using the measured CMB dipole moment (see section 3). Then, the magnification becomes

$$\mu|_{z_{\mathrm{CMB}}} = \frac{2}{aH\tilde{\chi}}(v_\parallel - v_{\parallel,\mathrm{CMB}})\,, \tag{2.7}$$

where the relevant quantity is now the velocity of the SN relative to the CMB rest frame. This simplifies the interpretation, since $v_\parallel - v_{\parallel,\mathrm{CMB}}$ is well described by linear perturbation theory. In fact, by performing the calculation in the CMB rest frame (as is normally done), we can set $\mathbf{v}_{\mathrm{CMB}} = 0$. The following relations will always assume that we work with CMB-frame redshifts and in the CMB rest frame.

It is straightforward to convert a perturbation in the luminosity distance (as in eq. (2.1)) into a perturbation of the SN magnitude from the homogeneous background value:

$$\delta m = -\frac{5}{2\ln 10}\,\mu \overset{z \ll 1}{=} -\frac{5}{\ln 10}\,\frac{\mathbf{v}\cdot\hat{\mathbf{n}}}{aH\tilde{\chi}}\,. \tag{2.8}$$

Note that this relation assumes that $\mu \ll 1$ and is thus not applicable at very low redshifts. While it is straightforward to derive the proper nonlinear relation for δm, this is not necessary for our purposes, since $z \gtrsim 0.01$ in our SN samples.

Now consider one object at redshift z_i in direction $\hat{\mathbf{n}}_i$ on the sky, and a second at $(z_j, \hat{\mathbf{n}}_j)$. We can derive the covariance of their residuals,

$$\begin{aligned} S_{ij} \equiv \langle \delta m_i \, \delta m_j \rangle &= \left[\frac{5}{\ln 10}\right]^2 \frac{a_i}{a_i' \chi_i} \frac{a_j}{a_j' \chi_j} \xi_{ij} \\ &= \left[\frac{5}{\ln 10}\right]^2 \frac{(1+z_i)^2}{H(z_i) d_L(z_i)} \frac{(1+z_j)^2}{H(z_j) d_L(z_j)} \xi_{ij} \,, \end{aligned} \tag{2.9}$$

where ξ_{ij} is the velocity covariance given by

$$\begin{aligned} \xi_{ij} \equiv \xi_{ij}^{\rm vel} &\equiv \langle (\mathbf{v}_i \cdot \hat{\mathbf{n}}_i)(\mathbf{v}_j \cdot \hat{\mathbf{n}}_j) \rangle \\ &= \frac{dD_i}{d\tau} \frac{dD_j}{d\tau} \int \frac{dk}{2\pi^2} P(k, a=1) \sum_\ell (2\ell+1) j_\ell'(k\chi_i) j_\ell'(k\chi_j) P_\ell(\hat{\mathbf{n}}_i \cdot \hat{\mathbf{n}}_j) \,. \end{aligned} \tag{2.10}$$

Here, primes denote derivatives of the Bessel functions with respect to their arguments, τ is the conformal time, $d\tau = dt/(a^2 H)$, D_i is the linear growth function evaluated at redshift z_i, and $\chi_i = \chi(z_i)$. The power spectrum $P(k, a)$ is evaluated in the present $(a = 1)$ and, at the large scales we are interested in, only the first $\simeq 10$ terms in the sum over the multipoles contribute. As mentioned above, we use velocities derived from linear theory and thus insert the linear matter power spectrum for our numerical results. We have verified that using a prescription for the nonlinear matter power spectrum in eq. (2.10) does not significantly affect our results. We thus conclude that the linear treatment is sufficient for our purposes. Physically, this is because the dominant contribution to the covariance comes from fairly large-scale modes. Note that in our approach, $\langle (\delta m_i)^2 \rangle$ is assumed to capture the random motion contribution to the variance of SN residuals.[2] While this is not expected to be completely accurate when using the linear matter power spectrum, the difference in the diagonal covariance elements is not very significant.[3]

We have denoted this covariance matrix $\mathbf{S}$ to emphasize that this is a cosmologically guaranteed "signal" to be added to the "noise" covariance matrix that accounts for the combination of statistical and systematic errors that affects SN distance measurements, such as intrinsic variations in the SN luminosity (see section 3). We again point out that the two geometric prefactors in eq. (2.9) each differ by an additive factor of 1 relative to those in [9] because we drop the term -2 in eq. (2.3) in order to achieve a consistent low-redshift expansion; we have checked that all neglected terms would contribute negligibly at $z \lesssim 0.1$.

2.2 Monopole subtraction

The magnification eq. (2.1) and its low-redshift version eq. (2.6) still have a monopole component, that is, a contribution that is uniform on the sky. However, since the SN magnitude

[2] An alternative approach by [17] models velocities with perturbation theory based on a density field derived from other surveys, and complements them with a "thermal" component of $\sim 150\,\mathrm{km/s}$ added in quadrature to account for nonlinearities. In contrast to our approach, this thus relies on external data sets. A detailed comparison between the covariances obtained using these different approaches would be interesting but is beyond the scope of this paper.

[3] For the low-redshift SNe we consider, nearly all of the redshifts are derived from host galaxy spectra, and so the motion of the SN within its host does not contribute to the residuals.

JCAP12(2015)033

residuals are defined with respect to the best-fit distance-redshift relation, this monopole is mostly absorbed in the fit. While there could technically be a residual monopole signal due to the fact that our fit (to a flat ΛCDM model, see section 4) is very restricted, we will assume here that the bulk of the monopole is removed. Thus, eq. (2.9) needs to be corrected.

To this end, we define the mean magnitude residual at redshift i as

$$\overline{\delta m}(z_i) = \int \delta m(z_i, \hat{\mathbf{n}})\, W(\hat{\mathbf{n}})\, d^2\hat{\mathbf{n}}\,, \tag{2.11}$$

where $W(\hat{\mathbf{n}})$ is the survey window function, which is normalized such that $\int W(\hat{\mathbf{n}})\, d^2\hat{\mathbf{n}} = 1$. Then, noting that we actually measure $\widehat{\delta m}_i = \delta m_i - \overline{\delta m}(z_i)$, the proper covariance is

$$S_{ij} \equiv \langle \widehat{\delta m}_i\, \widehat{\delta m}_j \rangle = \langle \left[\delta m(z_i, \hat{\mathbf{n}}_i) - \overline{\delta m}(z_i)\right] \left[\delta m(z_j, \hat{\mathbf{n}}_j) - \overline{\delta m}(z_j)\right] \rangle\,, \tag{2.12}$$

which can be worked out to be

$$\begin{aligned} S_{ij} = &\left[\frac{5}{\ln 10}\right]^2 \frac{(1+z_i)^2}{H(z_i) d_L(z_i)} \frac{(1+z_j)^2}{H(z_j) d_L(z_j)} \frac{dD_i}{d\tau} \frac{dD_j}{d\tau} \int \frac{dk}{2\pi^2} P(k, a=1) \\ &\times \sum_\ell (2\ell+1) j'_\ell(k\chi_i) j'_\ell(k\chi_j) \left[P_\ell(\hat{\mathbf{n}}_i \cdot \hat{\mathbf{n}}_j) - \frac{4\pi}{2\ell+1} \left[w_\ell(\hat{\mathbf{n}}_i) + w_\ell(\hat{\mathbf{n}}_j)\right] + 4\pi W_\ell \right], \end{aligned} \tag{2.13}$$

where the survey footprint has been expanded in spherical harmonics,

$$W(\hat{\mathbf{n}}) = \sum_{\ell m} w_{\ell m} Y_{\ell m}(\hat{\mathbf{n}})\,, \tag{2.14}$$

and the coefficients $w_\ell(\hat{\mathbf{n}}_i)$ and W_ℓ are defined as

$$w_\ell(\hat{\mathbf{n}}) \equiv \sum_m w_{\ell m} Y_{\ell m}(\hat{\mathbf{n}})\,, \qquad W_\ell \equiv \frac{\sum_m |w_{\ell m}|^2}{2\ell+1}\,. \tag{2.15}$$

The extra terms in the square brackets in eq. (2.13) are corrections due to the survey window. The W_ℓ are therefore just the angular power spectrum (more precisely, the "pseudo-C_ℓ") of the map, while $w_\ell(\hat{\mathbf{n}})$ is the ℓ portion of the survey mask at an arbitrary location. Note that, due to the required normalization of W, its value where the survey observes is not unity, but rather

$$W(\hat{\mathbf{n}}) = \begin{cases} \dfrac{1}{\Omega_{\rm sky}} & \text{(observed sky)} \\ 0 & \text{(unobserved sky).} \end{cases} \tag{2.16}$$

The term in the square parentheses in the last line of eq. (2.13), which includes the subtraction of the mean, is therefore a new result that has not, to our knowledge, been derived and included in previous analyses (although the existence of such a term has been pointed out in [9, 16]). For a full-sky window, it is easy to show that this term becomes $P_\ell(\hat{\mathbf{n}}_i \cdot \hat{\mathbf{n}}_j) - 1$ for $\ell = 0$ and remains equal to the original expression $P_\ell(\hat{\mathbf{n}}_i \cdot \hat{\mathbf{n}}_j)$ for the other multipoles.

We find that the monopole-subtracted formula leads to small but noticeable changes in the results, such as the constraints on the parameter A in section 5, and we recommend that it be used in future analyses.

3 SN Ia data and noise covariance

For our primary SN Ia dataset, we use the joint light-curve analysis (JLA) [18] of SNe from the Supernova Legacy Survey (SNLS) and the Sloan Digital Sky Survey (SDSS). JLA includes a recalibration of SNe from the first three years of SNLS [19, 20] along with the complete SN sample from SDSS, making it the largest combined SN analysis to date. The final compilation includes 740 SNe, $\sim$100 low-redshift SNe from several subsamples, $\sim$350 from SDSS at low to intermediate redshifts, $\sim$250 from SNLS at intermediate to high redshifts, and $\sim$10 high-redshift SNe observed with the Hubble Space Telescope.

We combine the individual covariance matrix terms provided[4] to compute the full covariance matrix, which includes statistical errors (correlated uncertainties in the light-curve measurements, intrinsic scatter, lensing dispersion) and a variety of systematic errors (photometric calibration, uncertainty in the bias correction, light-curve model uncertainty, potential non-Ia contamination, uncertainty in the Milky Way dust extinction correction, and uncertainty in the host galaxy correction).

Although we compute the covariance matrix as described in the JLA analysis, we leave out two contributions to the total error. First, we leave out the additional scatter of $150\,\mathrm{km/s} \times 5/(cz \ln 10)$ added in quadrature to the other statistical errors on the diagonal to account for peculiar velocity. This peculiar velocity scatter does not apply because peculiar velocities are not a source of noise in our analysis; instead, they are modeled by the formalism discussed in section 2. We also leave out the systematic error term corresponding to uncertainty in the peculiar velocity *correction* applied to the low-z JLA redshifts. Since our aim is to study the peculiar velocities themselves, we want to avoid this correction and then leave out the systematic error associated with it. To this end, we obtain the CMB-frame redshifts z_{CMB} directly from the measured heliocentric redshifts z_{hel}. Specifically, for each SN we compute

$$1 + z_{\mathrm{CMB}} = (1 + z_{\mathrm{hel}}) \left[1 + \frac{v_{\mathrm{CMB}}}{c} \left(\hat{\mathbf{n}}_{\mathrm{CMB}} \cdot \hat{\mathbf{n}} \right) \right], \tag{3.1}$$

where $\hat{\mathbf{n}}$ is the sky position of the SN, $\hat{\mathbf{n}}_{\mathrm{CMB}}$ is the CMB dipole direction, and v_{CMB} is the velocity of the Solar System barycenter relative to the CMB rest frame implied by the dipole amplitude. We use the measured values $v_{\mathrm{CMB}} = 369\,\mathrm{km/s}$ and $\hat{\mathbf{n}}_{\mathrm{CMB}} \equiv (l, b) = (263.99^\circ, 48.26^\circ)$, where the quoted uncertainties [21] are negligible for our purposes.

For comparison, we separately consider the Union2 SN Ia analysis [22] from the Supernova Cosmology Project.[5] We use the full covariance matrix provided for the Union2 SN magnitudes, but as with JLA, we remove the peculiar velocity scatter (300 km/s here) that was added to the diagonal. The redshifts given for the Union2 SNe are just the heliocentric redshifts transformed to the CMB rest frame, so we use them directly.

Note that the Union2 compilation of 557 SNe has been superseded by the Union2.1 compilation [23] of 580 SNe, but here the goal is a fair comparison to previous work that analyzes the Union2 data. Since the primary change in Union2.1 is the addition of a set of high-redshift SNe, and since only low-redshift SNe are relevant for our analysis, we would expect the two compilations to produce very similar results. When substituting Union2.1 for Union2, our results do not change qualitatively, but there are some minor differences due to new estimates for some corrected SN magnitudes and their errors. Union2.1 also includes a

[4]http://supernovae.in2p3.fr/sdss_snls_jla/.

[5]http://supernova.lbl.gov/Union/.

JCAP12(2015)033

host-mass correction (see below) that Union2 does not, but this is relatively small and only accounts for part of the magnitude differences.

Finally, we briefly consider the low-z compilation from the older analysis of [24], also for comparison with other work. This compilation does not include an analysis of systematic errors, so the uncertainty in a SN magnitude is just a combination of the light-curve measurement errors and the derived intrinsic scatter of $\sigma_{\rm int} = 0.08\,$mag. Again, we do not include the peculiar velocity scatter of 300 km/s prescribed for a cosmological analysis. Although CMB-frame redshifts are given, we transform the given heliocentric redshifts into CMB-frame redshifts ourselves using eq. (3.1).

Because SNe Ia are not perfect standard candles, it is necessary to correct the observed peak magnitude of each SN for the empirical correlations between the SN Ia absolute magnitude and both the stretch (broadness) and color measure associated with the light-curve fitter. More recently, it has become common to fit for a constant offset in the absolute magnitude for SNe in high-stellar-mass host galaxies. For JLA, the corrected magnitude is therefore given by

$$m^{\rm corr} = m + \alpha \times (\text{stretch}) - \beta \times (\text{color}) + P\,\Delta M\,, \tag{3.2}$$

where α, β, and ΔM are nuisance parameters describing, respectively, the stretch, color, and host-mass corrections. The measured $P \equiv P(M_* > 10^{10} M_\odot)$ is the probability that the SN occurred in a high-stellar-mass host galaxy. Note that, as mentioned above, Union2 does not include this host-mass correction; also, the analysis of [24] uses a different light-curve fitter with different (but related) light-curve corrections.

For each of the three datasets, we fix the SN Ia nuisance parameters to their best-fit values from a fit to the Hubble diagram (for JLA, we perform this fit and correct the magnitudes ourselves; for the other datasets, we use precorrected magnitudes). In a proper cosmological analysis, one should vary the SN nuisance parameters simultaneously with any cosmological parameters. In practice, however, the nuisance parameters are well-constrained by the Hubble diagram with little dependence on the cosmological model, so holding them fixed should be a good approximation, especially for our purposes here.

4 Likelihood

We write the full covariance $\mathbf{C}$ as the sum of two contributions, $\mathbf{C} = \mathbf{S} + \mathbf{N}$, where $\mathbf{S}$ is the signal covariance, dominated by velocities at low z and discussed in section 2, and $\mathbf{N}$ is the noise covariance, described in section 3.

Assuming a given cosmological model that allows us to calculate $\mathbf{S}$ (eq. (2.9)), the *optimal* way to determine whether the data favors peculiar velocities is to consider evidence for the detection of the full signal matrix $\mathbf{S}$. This approach uses more information in the data than the search for any particular moment, such as the dipole, of the peculiar velocity field.

Here we would like to detect evidence for coherent departures of supernova magnitudes from the mean — that is, clustering. To do this, we introduce a new dimensionless parameter A and let $\mathbf{S} \to A\,\mathbf{S}$, where $A = 1$ for the fiducial model. $A = 0$ corresponds to the case that magnitude residuals are purely due to noise and systematics in the SN Ia data. We would like to test whether A is consistent with one and different from zero. Including the new parameter A, the full covariance becomes

$$\mathbf{C} = A\,\mathbf{S} + \mathbf{N}\,, \tag{4.1}$$

where $0 \le A < \infty$.

On the other hand, allowing for an excess bulk flow component is interesting as well, as it can be used to search for signatures beyond the fiducial ΛCDM model and also allows us to compare our results with the existing literature (see section 6). In this case, the magnitude residuals are affected by an additional bulk velocity $\mathbf{v}_{\rm bulk}$ (e.g. [9]):

$$\Delta m_i^{\rm bulk} \equiv \Delta m^{\rm bulk}(\mathbf{v}_{\rm bulk}; z_i, \hat{\mathbf{n}}_i) = -\left(\frac{5}{\ln 10}\right) \frac{(1+z_i)^2}{H(z_i) d_L(z_i)} \hat{\mathbf{n}}_i \cdot \mathbf{v}_{\rm bulk}\,, \tag{4.2}$$

where z_i and $\hat{\mathbf{n}}_i$ are the redshift and sky position of the SN, while $\mathbf{v}_{\rm bulk}$ is a fixed three-dimensional vector. In the quasi-Newtonian picture, $\mathbf{v}_{\rm bulk}$ corresponds to the bulk motion of the SN sample; however, in the context of non-standard cosmological models (such as those breaking homogeneity or isotropy), this should really be seen as a convenient parametrization of the dipole of SN magnitude residuals.

Putting these ingredients together, we construct a multivariate Gaussian likelihood[6]

$$\mathcal{L}(A, \mathbf{v}_{\rm bulk}) \propto \frac{1}{\sqrt{|\mathbf{C}|}} \exp\left[-\frac{1}{2} \mathbf{\Delta m}^{\intercal} \mathbf{C}^{-1} \mathbf{\Delta m}\right], \tag{4.3}$$

where the elements of the vector $\mathbf{\Delta m}$ are

$$(\mathbf{\Delta m})_i = m_i^{\rm corr} - m^{\rm th}(z_i, \mathcal{M}, \Omega_m) - \Delta m_i^{\rm bulk}(\mathbf{v}_{\rm bulk})\,, \tag{4.4}$$

where $m_i^{\rm corr}$ are the observed, corrected magnitudes and $m^{\rm th}(z_i, \mathcal{M}, \Omega_m)$ are the theoretical predictions for the background cosmological model (see below). The $\mathcal{M}$ parameter corresponds to the (unknown) absolute calibration of SNe Ia; we analytically marginalize over it in all analyses (e.g. appendix of [25]).

We emphasize that, since the covariance depends on the parameter A that we are interested in constraining, we need to include a term for the $1/\sqrt{|\mathbf{C}|}$ prefactor in addition to the usual χ^2 quantity. Since the covariance is a strictly increasing function of A, neglecting the prefactor would lead to the clearly erroneous result that the likelihood is a maximum for $A \to \infty$.

The likelihood in eq. (4.3) is the principal tool we will use for our analyses. In this most general form, the likelihood depends on two input quantities (four parameters, since the velocity has three components): the normalization A of the signal component of the covariance matrix and the excess bulk velocity $\mathbf{v}_{\rm bulk}$ not captured by the velocity covariance. Note that, in the fiducial model, $A = 1$ and $\mathbf{v}_{\rm bulk} = 0$.

Throughout our analyses, we assume a flat ΛCDM model ($w = -1$, $\Omega_k = 0$) with free parameters fixed to values consistent with data from *Planck* [26] and other probes. That is, we fix $\Omega_m = 0.3$, physical matter density $\Omega_m h^2 = 0.14$, physical baryon density $\Omega_b h^2 = 0.0223$, scalar spectral index $n_s = 0.965$, and amplitude of scalar fluctuations $A_s = 2.22 \times 10^{-9}$. The corresponding derived value of the Hubble constant is $h = 0.683$, and that of the amplitude of mass fluctuations is $\sigma_8 = 0.79$. Within the ΛCDM model, these parameters are determined very precisely using *Planck* data alone, and we have explicitly checked that modest changes in the cosmological model, larger than those allowed by *Planck*, have a negligible effect on

[6]Note that SN flux, or a quantity linearly related to it, might be a better choice for the observable than the magnitude, given that we expect the error distribution of the former to be more Gaussian than the latter. Nevertheless, this choice should not impact our results, as the fractional errors in flux are not too large, and we have explicitly checked that the distribution of the observed magnitudes around the mean is approximately Gaussian. Therefore we follow most literature on the subject and work directly with magnitudes.

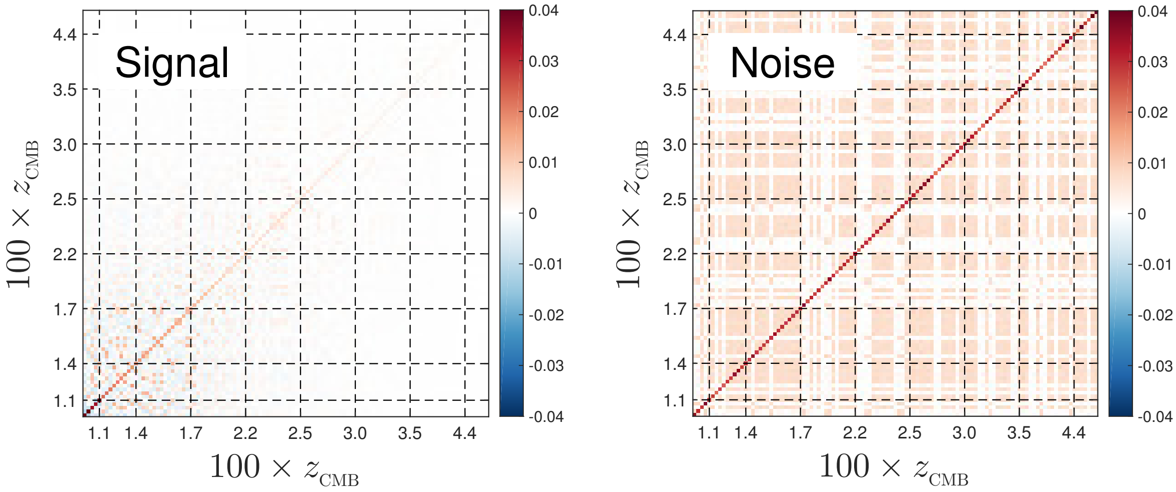

Figure 1. Comparison of the signal (left panel) and noise (right panel) contributions to the full covariance matrix for the 111 SNe at $z < 0.05$ from the JLA compilation.

our results. We can therefore conclude that adding *Planck* priors and marginalizing over these parameters would not significantly affect our constraints. This is not surprising. The background cosmology only affects the monopole of the Supernova magnitudes, and even this dependence is weak at very low redshifts (since we marginalize over $\mathcal{M}$). Only a much larger change in the parameters would affect the expected pairwise covariance, which we do not expect to be able to measure precisely in the first place.

In figure 1, we compare the noise covariance $\mathbf{N}$ to the signal covariance $\mathbf{S}$ for our fiducial cosmology. While the noise contribution is typically larger than the signal, the signal is not negligible, and it actually dominates for the lowest-redshift SNe. The noise, unlike the signal, becomes effectively smaller as more SNe are used in the analysis, making the signal important for the whole redshift range considered (see also the discussion in [27]).

5 Constraints on the amplitude of signal covariance

We first consider whether the data itself shows a preference for the presence of the velocity (signal) covariance. Therefore, we explore the constraints on A using the likelihood in eq. (4.3) and fixing $\mathbf{v}_{\rm bulk} = 0$.

The constraints on the parameter A, which determines the fraction of the velocity covariance added to the full covariance $\mathbf{C}$, are shown in figure 2, with the numerical results given in table 1. We have adopted a uniform prior on A such that our Bayesian posterior is proportional to the likelihood in eq. (4.3). All data choices consistently use the available SNe out to $z = 0.05$. This leaves 111 objects in the JLA analysis and 132 in the Union2 analysis. We have explicitly checked that the results are insensitive to the precise redshift cutoff; they are driven by the lowest-redshift SNe, and $z < 0.05$ comfortably captures all of them.

The solid black curve shows JLA, the most current and rigorously calibrated dataset. JLA does not rule out the $A = 0$ hypothesis; in fact, the likelihood peaks near this value. Nevertheless, JLA is fully consistent with the standard value $A = 1$, with a probability of 0.07 for $A > 1$.

JCAP12(2015)033

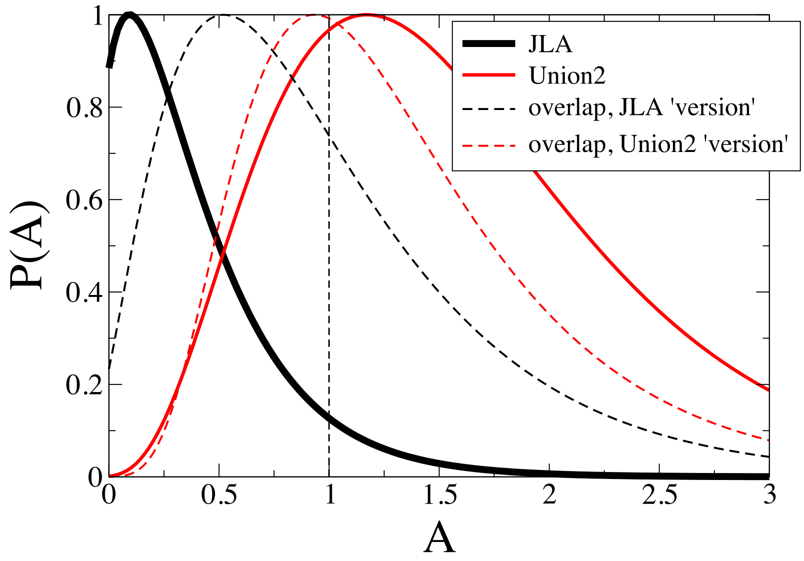

Figure 2. Constraints on the parameter A that quantifies the amount of velocity correlations ($A = 1$ is the standard ΛCDM value). The JLA data are consistent with $A = 1$ but do not rule out the noise-only hypothesis $A = 0$. JLA and Union2 give somewhat different constraints, though they are not statistically inconsistent. Note that differences remain even after restricting to the rather large subset of SNe that they have in common (dashed lines).

	$P(A)$ (figure 2)				$v_{\rm bulk}^{\rm max\text{-}like}$ (figure 3)		$v_{\rm bulk}^{\rm angle\text{-}avg}$ (figure 4)
Survey	ML	95% C.L.	$\Delta\chi^2\|_{A=0}$	$\Delta\chi^2\|_{A=1}$	ML	95% C.L.	95% C.L.
JLA	0.19	$(0, 1.15)$	0.24	4.13	187	$(-108, 485)$	$(0, 376)$
Union2	1.19	$(0.19, 3.27)$	13.2	0.07	265	$(-37, 568)$	$(0, 456)$

Table 1. Summary of numerical results. For both JLA and Union2, we show the best-fit, maximum-likelihood (ML) values and 95% confidence intervals for A. We also show the quantity $\Delta\chi^2$ (that is, $-2\Delta \ln L$) between the best-fit value and special values $A = 0$ (no velocity signal) and $A = 1$ (ΛCDM velocity signal). We also show ML and 95% intervals for bulk velocity in the best-fit direction and 95% intervals for angle-averaged bulk velocity (here we do not report ML values, which are near zero). All velocities are in units of km/s.

The solid red curve shows the result from the Union2 dataset. While it is noticeably different than the JLA result, the two likelihoods are mutually consistent; in particular, $A = 1$ is a satisfactory fit to both. Nevertheless, Union2 is different in that it strongly disfavors $A = 0$.

In order to gain additional insight into the difference between the two datasets, we have identified SNe at $z < 0.05$ that overlap between the two datasets, a total of 96 objects. Performing the analysis on this overlap (dashed lines in figure 2), we see that the results are in better agreement but still somewhat disagree, despite both analyses using the same SN set. Part of the reason is that JLA and Union2 determine the magnitudes differently; however, even some redshifts do not match. We find a root-mean-square (rms) redshift difference of 1.4% for the object-to-object comparison of the 96 overlapping SNe, and the largest difference is 5%. A further exploration of precisely why the SN redshifts and magnitudes differ is beyond the scope of this study, but we have explicitly checked that the difference between JLA and Union2 for the overlap set is largely due to differences in the estimated apparent magnitudes, not the redshifts.[7]

We also make connection to previous work in [28], where the first cosmological constraints from the correlations of SN Ia peculiar velocities have been obtained. Instead of parametrizing the covariance with a multiplicative amplitude, they jointly constrained the cosmological parameters Ω_m and σ_8. Using the earlier SN dataset from [24], they found constraints broadly consistent with ΛCDM values. Using the same dataset, we roughly agree with [28], our likelihood favoring $A \simeq 1.4$ with a large uncertainty but effectively ruling out $A = 0$. However, we note that the dataset of [24] includes some SNe with extremely low redshifts (as low as $z = 0.002$), which are not in the Hubble flow and for which the assumption of small residuals in eq. (2.8) breaks down (see also discussion after eq. (2.10)). Objects at such extremely low redshifts are mutually separated by distances of a few tens of Mpc; their relative velocities are therefore expected to have important nonlinear corrections, in addition to the linear relation eq. (2.8) breaking down, and the analysis would have to be carefully generalized to take this into account. When we exclude all SNe with $z < 0.01$ from the dataset of [24], the likelihood for A actually looks very similar to the JLA constraints in figure 2, favoring $A = 0$ but still statistically consistent with $A = 1$.

To summarize, we find that JLA, the most current and rigorous dataset, does not favor the presence of SN velocity covariance guaranteed in the ΛCDM model, but is nonetheless consistent with it. We also find that there is considerable variation in the SN data in terms of their constraints on the velocity covariance, and in particular that the optimistic-looking results found in [28] were due to some very-low-redshift SNe that may be too nearby for accurate modeling with linear theory.

The covariance of SN flux residuals has the potential to provide additional information about cosmological parameters and other interesting physics [29–33]. Our results suggest that current data do not yield interesting constraints. This will likely change with larger, homogeneous samples with greater sky coverage, such as those expected from the Large Synoptic Survey Telescope (LSST), currently under construction.

6 Constraints on excess bulk velocity

The optimal way to search for the effect of SN velocity correlations in the context of a fiducial cosmological model is to test for the presence of the full signal covariance, as we did in section 5. However, we can also use the SN magnitude residuals to search for a dipolar distortion (for example, due to bulk motion) beyond what is expected in ΛCDM. This provides constraints on physics beyond the concordance cosmology, such as a breaking of statistical isotropy or homogeneity, or the presence of a single large long-wavelength perturbation. The search for bulk flows is the subject of a significant body of literature. Here we use a different approach, and we make the connection to previous literature in the next section.

Bulk velocity is usually defined as the motion of the volume spanned by SNe Ia and the rest frame defined by the CMB. Moving the SN redshifts to the CMB frame, we are looking for an overall motion between the SN volume and the rest frame. Since we aim to search for an excess bulk flow *beyond* ΛCDM, we include the velocity correlations $\mathbf{S}$ in the likelihood,

[7] We have checked that the sky positions of JLA and Union2 overlapping SNe do precisely agree. We have also found that the subset of these SNe that are also found in the sample of [24] — 40 in total — have redshifts that mostly agree very well with JLA, but show larger discrepancies with Union2.

JCAP12(2015)033

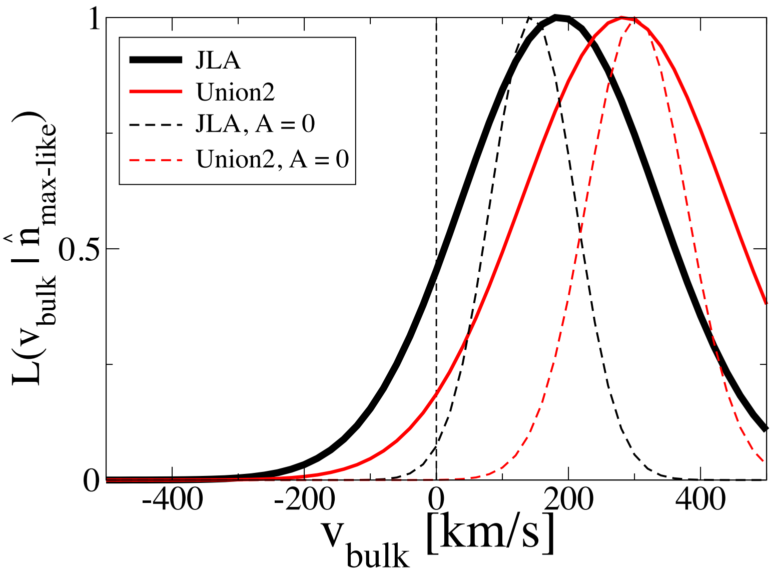

Figure 3. A slice through the 3D likelihood for excess bulk velocity. The direction is fixed to be $\hat{\mathbf{n}}_{\text{max-like}}$ (different for each dataset), while the amplitude of the dipole is varied and allowed to be positive or negative. Conclusions about the bulk flow would differ significantly if the velocity signal covariance were set to zero (dashed lines), as in most previous work on the subject.

fixing $A = 1$. Since $\mathbf{S}$ includes all velocity correlations within ΛCDM, including the dipole, we expect the posterior for the bulk flow to be consistent with zero if ΛCDM provides a good description of the SN data. Of course, this assumes that our linear modeling of the velocity correlations is accurate for the SN sample and also that there are no unaccounted-for systematic errors in the SN data that could masquerade as an excess bulk flow.

For this analysis, we therefore adopt the likelihood from eq. (4.3), setting $A = 1$ but allowing the bulk velocity $\mathbf{v}_{\text{bulk}} = (v_{\text{bulk}}, \theta, \phi)$ to vary in magnitude and direction. In order to get a sense of the three-dimensional likelihood $\mathcal{L}(v_{\text{bulk}}, \theta, \phi)$, we first consider the likelihood of the excess bulk flow amplitude in a cut through the best-fit direction, that is, as a function of v_{bulk} with θ and ϕ set to their maximum-likelihood values. This is shown in figure 3, and note that we continue the scan past zero velocity in the direction opposite that of the best fit by letting the amplitude of the bulk flow take negative values. Because the likelihood is Gaussian, and because $\mathbf{v}_{\text{bulk}}$ enters the observable magnitude linearly (see eq. (4.2)), the likelihood of the bulk velocity is also guaranteed to be Gaussian. Therefore, the likelihood ratio between the best-fit $(v_{\text{bulk}}, \theta, \phi)$ and $v_{\text{bulk}} = 0$ immediately translates into the confidence at which zero excess bulk velocity is ruled out, assuming uniform priors on each component of the vector $\mathbf{v}_{\text{bulk}}$.

Figure 3 shows that, once the velocity covariance is properly taken into account, SN data do not favor any bulk velocity beyond the amount expected in ΛCDM. For example, the JLA likelihood peaks at $(v_{\text{bulk}}, l, b) = (187\,\text{km/s}, 323°, 25°)$, but this likelihood is larger than that for $v_{\text{bulk}} = 0$ only by $-2\Delta \ln \mathcal{L} = -1.6$, far too low even for 68.3% (1σ) evidence, which in three dimensions would be $-2\Delta \ln \mathcal{L} \simeq -3.5$.

We would now like to explicitly calculate the posterior distribution of the amplitude of an excess bulk velocity. Assuming uniform priors on each component of $\mathbf{v}_{\text{bulk}}$ would produce an additional v_{bulk}^2 factor in the posterior, driving it to zero for the $v_{\text{bulk}} = 0$ case so that

JCAP12(2015)033

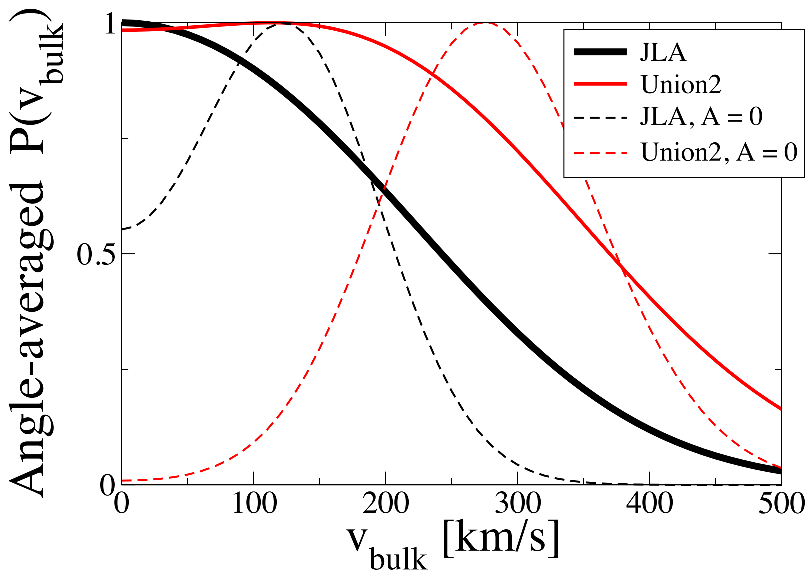

Figure 4. Angle-averaged posterior on the amplitude of bulk velocity in excess of the correlations captured by the full ΛCDM velocity covariance. Both JLA and Union2 data are consistent with zero velocity, with relatively large error. The conclusion would again be very different if the velocity covariance were artificially set to zero (dashed lines).

$\mathbf{v}_{\rm bulk} = 0$ is automatically ruled out. An alternative that allows us to test the $\mathbf{v}_{\rm bulk} = 0$ assumption, implicitly (or explicitly [34]) adopted by most previous work, is to choose the prior $\Pr(v_{\rm bulk}) \propto 1/v_{\rm bulk}^2$ or, alternatively, to consider the angle-averaged likelihood

$$P^{\text{angle-averaged}}(\mathbf{v}_{\rm bulk}) \propto \int \mathcal{L}(\mathbf{v}_{\rm bulk})\, d\cos\theta\, d\phi\,. \tag{6.1}$$

We plot this likelihood in figure 4. It is immediately apparent that both JLA and Union2 data show no preference for excess bulk velocity, though there is a large uncertainty. Performing the same analysis but setting the velocity correlations to zero (so that $\mathbf{C} = \mathbf{N}$ with $\mathbf{S} = 0$), the results are drastically different, favoring bulk flows of several hundred km/s and, in the case of Union2, firmly ruling out the $v_{\rm bulk} = 0$ case. This is in agreement with the conclusion found in previous work [35–40]. In the dashed curves shown in figure 4, we have not included the 150 km/s (300 km/s) scatter that is added in quadrature to the diagonal of the noise covariance $\mathbf{N}$ for JLA (Union2) data in some analyses. This clearly does not capture the significant full covariance of SN residuals due to large-scale structure. However, when adding back this contribution, we find nearly perfect agreement with the results of [37].

Given the importance of this issue, we stress again that the dashed lines in figures 3 and 4 *do not show the proper likelihood of any peculiar velocity*, ΛCDM or otherwise, since a guaranteed component of the covariance of the data has been neglected (nevertheless, one can still use these incorrect likelihoods to construct an estimator for bulk flow, which we will turn to in the next section). Since the velocity covariance $\mathbf{S}$ gives a guaranteed source of correlations in ΛCDM, we argue that it should always be included in likelihood analyses of SN magnitude residuals. Neglecting this covariance will lead to suboptimal estimators and, in general, biased results.

7 Relation to previous bulk flow measurements

A significant body of earlier work on SN velocities neglected the velocity covariance (and the lensing covariance, which is important at higher redshifts). These analyses often found evidence for non-zero bulk flow, and we confirm these findings with our dashed curves in figures 3 and 4. This bulk velocity with $A = 0$ is difficult to interpret, since it was obtained in an analysis with a guaranteed contribution to the covariance of the observables artificially set to zero.

Nevertheless, one can derive a theoretical expectation for what one should expect for the bulk velocity derived in this way; we call it $\mathbf{v}_{\rm bulk}^{\rm noise\text{-}only}$, and in some previous work it corresponds to what the authors simply call "bulk velocity". Note that this is not the *excess* bulk velocity over the ΛCDM expectation considered in the previous sections.

We will adopt the likelihood from eq. (4.3) once more, but we define a new vector $\mathbf{x}$ via $\mathbf{\Delta m}^{\rm bulk}(\mathbf{v}_{\rm bulk}) \equiv v_{\rm bulk}\,\mathbf{x}$, where

$$x_i \equiv -\left(\frac{5}{\ln 10}\right)\frac{(1+z_i)^2}{H(z_i)d_L(z_i)}\,\hat{\mathbf{n}}_i\cdot\hat{\mathbf{n}}_{\rm bulk}\,. \tag{7.1}$$

To estimate $v_{\rm bulk}^{\rm noise\text{-}only}$, we set the signal covariance to zero, assume a fixed direction $\hat{\mathbf{n}}_{\rm bulk}$, and find the maximum of the likelihood; that is

$$\widehat{v}_{\rm bulk}^{\rm noise\text{-}only} \longleftrightarrow \max_{v_{\rm bulk}}\left[\mathcal{L}(A=0,\mathbf{v}_{\rm bulk})\right]. \tag{7.2}$$

Maximizing with respect to $v_{\rm bulk}$, one finds

$$\widehat{v}_{\rm bulk}^{\rm noise\text{-}only} = \frac{\mathbf{y}^\intercal\,\delta\mathbf{m}}{\mathbf{y}^\intercal\,\mathbf{x}}\,, \tag{7.3}$$

where we have defined for convenience a new vector $\mathbf{y}$ as $\mathbf{y} \equiv \mathbf{N}^{-1}\mathbf{x}$, and where $\delta\mathbf{m}$ is the vector of SN magnitude residuals (eq. (4.2) without the $\Delta m^{\rm bulk}$ term). Assuming ΛCDM, and still keeping the direction $\hat{\mathbf{n}}_{\rm bulk}$ fixed, the expected (mean) velocity is of course zero since $\langle\delta m_i\rangle = 0$.

We are more interested in the variance of this quantity, which can be computed directly and is equal to

$$\langle(\widehat{v}_{\rm bulk}^{\rm noise\text{-}only})^2\rangle = \frac{\mathbf{y}^\intercal(\mathbf{S}+\mathbf{N})\,\mathbf{y}}{(\mathbf{y}^\intercal\,\mathbf{x})^2}\,, \tag{7.4}$$

since the true SN magnitude covariance for ΛCDM is the sum of both signal and noise: $\langle(\delta m_i)(\delta m_j)\rangle = S_{ij} + N_{ij}$. The square root of this quantity is the desired theoretical expectation for the rms bulk velocity in ΛCDM when one ignores the signal covariance matrix.

Using the JLA SNe up to redshift $z = 0.05$, the ΛCDM expectation for the rms velocity varies from about 150–170 km/s as a function of $\hat{\mathbf{n}}_{\rm bulk}$, with a sky-averaged value of 162 km/s. Assuming only noise in the data, $\langle(\delta m_i)(\delta m_j)\rangle = N_{ij}$, the result is 71 km/s. The Union2 data give similar results.

We have therefore found that the predicted rms value of $v_{\rm bulk}^{\rm noise\text{-}only}$, assuming ΛCDM and SN data up to $z = 0.05$, is $\sim$160 km/s, and that nearly half of this value would be generated by statistical scatter in SN magnitudes in the absence of any peculiar velocities in the universe (such a contribution is sometimes referred to as the "noise bias"). The peak of the JLA likelihood (black dashed line in figure 4) is in agreement with the ΛCDM expectation;

JCAP12(2015)033

Union2 gives a somewhat larger result. Again, however, we caution that the analysis in this section is suboptimal, given that we do condense the data into a weighted dipole estimator $\widehat{v}_{\rm bulk}^{\rm noise\text{-}only}$ rather than using the full covariance. Moreover, this estimator is significantly affected by noise bias which needs to be subtracted. Given the uncertainties in the noise covariance, the subtraction of noise bias will lead to additional systematic uncertainties in the actual peculiar velocity measurement.

We have not attempted to repeat the analyses of some past work that studied the velocity field of low-redshift SNe [38–45] or the anisotropy of the universe from the distribution of nearby SN distances [46–51], since these studies adopted a wide variety of approaches and, in some cases, complicated statistical procedures whose results are calibrated on simulations. We emphasize, however, that the velocity covariance due to large-scale structure should be included in any such analyses in order to obtain unbiased results and draw reliable statistical conclusions about the velocity field of the nearby universe.

8 Conclusions

In this paper we have revisited the constraints on bulk velocity — the relative motion of the volume populated by nearby SNe Ia and the rest frame defined by the CMB. Our emphasis was on a precise and clear procedure for selecting the data, performing the analysis, and modeling the theoretical expectation. We concentrated on SNe Ia as tracers of cosmic structure and studied two separate (but overlapping) datasets. Our methodology applies equally well to galaxies and other tracers of large-scale structure.

We argued, and demonstrated with explicit calculations, that inclusion of the "signal" covariance matrix that captures the peculiar velocity correlations between SNe is crucial. The velocities provide a guaranteed source of covariance between SNe; while the velocity contribution is subdominant compared to the noise except at the lowest redshifts (see figure 1), it does not become smaller as more SNe are included in the analysis. Neglecting the velocity covariance, as done by a significant body of earlier work on SN velocities and tests of statistical isotropy, leads to results that are both biased and difficult to interpret.

Our approach was based on a likelihood that includes both the signal and noise covariance and four free parameters: the normalization A, specifying the fraction of the signal added to the covariance, and three components of an excess bulk velocity $\mathbf{v}_{\rm bulk}$ beyond that which is encoded in the signal covariance. For the fiducial ΛCDM model, $A = 1$ and $\mathbf{v}_{\rm bulk} = 0$.

We first investigated whether the standard ΛCDM velocity covariance ($A = 1$) is preferred over the case in which the covariance is ignored ($A = 0$); that is, we constrained $\mathcal{L}(A, \mathbf{v}_{\rm bulk} = 0)$. We found that the JLA dataset, while consistent with $A = 1$, cannot rule out $A = 0$, and in fact its likelihood peaks near zero (figure 2). Therefore, we did not find convincing evidence in the data for the correlations expected from velocities. Although we expect things to change with future data, when precise measurements of a quantity like A will effectively constrain cosmological parameters such as Ω_m and σ_8, our results indicate that current data are not close to providing such useful constraints.

We then pursued a different approach; we assumed a standard ΛCDM velocity covariance (the $A = 1$ case) and tested for excess bulk velocity $\mathbf{v}_{\rm bulk}$ beyond that already captured by the covariance — that is, we adopted the likelihood $\mathcal{L}(A = 1, \mathbf{v}_{\rm bulk})$ in the analysis. We found that current SN data provide no evidence for a departure from the null hypothesis $\mathbf{v}_{\rm bulk} = 0$ (figures 3 and 4). This result is in sharp contrast to the inference one would have

JCAP12(2015)033

made by ignoring the velocity covariance (that is, setting $A = 0$ in the same analysis), as some previous analyses in the literature have done.

To better understand this latter case, we separately studied inferred constraints on a "non-excess" bulk velocity where the velocity covariance has been ignored — that is, the $\mathcal{L}(A = 0, \mathbf{v}_{\rm bulk}^{\rm noise\text{-}only})$ case. Note that this bulk velocity is more difficult to interpret since it was obtained by ignoring a guaranteed source of correlations in the data. We showed that the rms of the estimated $v_{\rm bulk}^{\rm noise\text{-}only}$, assuming ΛCDM and SN data up to $z = 0.05$, is expected to be $\sim 160\,{\rm km/s}$, and that nearly half of this value would be generated by a contribution purely from intrinsic and observational scatter in the SN magnitudes. Therefore, there are really two problems with this approach: not only is the constrained quantity difficult to interpret, but it is also guaranteed to be nonzero even without any peculiar velocities in the universe, which is clearly not optimal for cosmological interpretations.

The mapping of velocities in the universe using nearby tracers of large-scale structure has had a remarkably long and productive history. With upcoming large-field, fast-scanning surveys, it is likely that data will become of sufficiently high quality to enable peculiar velocities to progress to the next level and become competitive cosmological probes. Of course, data analysis and theoretical modeling will have to progress as well. In this paper we have demonstrated that, even for current data, clearly defining the quantities to be constrained and carefully accounting for the guaranteed correlations between objects due to large-scale structure are two factors of key importance.

Acknowledgments

We thank Alex Conley, De-Chang Dai, Vera Gluščević, Chris Gordon, Will Kinney, Yin-Zhe Ma, and Anže Slosar for useful discussions and Greg Aldering, Mike Hudson, and Alex Kim for comments on an earlier draft of this paper. We also thank the anonymous referee for useful comments. DH and DLS are supported by NSF under contract AST-0807564 and DOE under contract DE-FG02-95ER40899. DH has also been supported by the DFG Cluster of Excellence "Origin and Structure of the Universe" (http://www.universe-cluster.de/).

References

[1] N. Kaiser, *Theoretical implications of deviations from Hubble flow*, *Mon. Not. Roy. Astron. Soc.* **231** (1989) 149 [INSPIRE].

[2] K.M. Gorski, M. Davis, M.A. Strauss, S.D.M. White and A. Yahil, *Cosmological velocity correlations — observations and model predictions*, *Astrophys. J.* **344** (1989) 1.

[3] A. Sandage, G.A. Tammann and A. Yahil, *The velocity field of bright nearby galaxies. I. The variation of mean absolute magnitude with redshift for galaxies in a magnitude-limited sample*, *Astrophys. J.* **232** (1979) 352 [INSPIRE].

[4] A. Nusser and M. Davis, *The cosmological bulk flow: consistency with ΛCDM and $z \approx 0$ constraints on σ_8 and γ*, *Astrophys. J.* **736** (2011) 93 [arXiv:1101.1650] [INSPIRE].

[5] E. Macaulay et al., *Power spectrum estimation from peculiar velocity catalogues*, *Mon. Not. Roy. Astron. Soc.* **425** (2012) 1709 [arXiv:1111.3338] [INSPIRE].

[6] E. Branchini, M. Davis and A. Nusser, *The velocity field of 2MASS Redshift Survey $K_s = 11.75$ galaxies: constraints on β and bulk flow from the luminosity function*, *Mon. Not. Roy. Astron. Soc.* **424** (2012) 472 [arXiv:1202.5206] [INSPIRE].

[7] M. Feix, A. Nusser and E. Branchini, *Tracing the cosmic velocity field at $z \sim 0.1$ from galaxy luminosities in the SDSS DR7*, JCAP **09** (2014) 019 [arXiv:1405.6710] [INSPIRE].

[8] M.A. Strauss and J.A. Willick, *The density and peculiar velocity fields of nearby galaxies*, Phys. Rept. **261** (1995) 271 [astro-ph/9502079] [INSPIRE].

[9] L. Hui and P.B. Greene, *Correlated fluctuations in luminosity distance and the importance of peculiar motion in supernova surveys*, Phys. Rev. **D 73** (2006) 123526 [astro-ph/0512159] [INSPIRE].

[10] T.M. Davis et al., *The effect of peculiar velocities on supernova cosmology*, Astrophys. J. **741** (2011) 67 [arXiv:1012.2912] [INSPIRE].

[11] C. Bonvin, R. Durrer and M.A. Gasparini, *Fluctuations of the luminosity distance*, Phys. Rev. **D 73** (2006) 023523 [*Erratum ibid.* **D 85** (2012) 029901] [astro-ph/0511183] [INSPIRE].

[12] A. Challinor and A. Lewis, *The linear power spectrum of observed source number counts*, Phys. Rev. **D 84** (2011) 043516 [arXiv:1105.5292] [INSPIRE].

[13] C. Bonvin and R. Durrer, *What galaxy surveys really measure*, Phys. Rev. **D 84** (2011) 063505 [arXiv:1105.5280] [INSPIRE].

[14] F. Schmidt and D. Jeong, *Cosmic rulers*, Phys. Rev. **D 86** (2012) 083527 [arXiv:1204.3625] [INSPIRE].

[15] D. Jeong, F. Schmidt and C.M. Hirata, *Large-scale clustering of galaxies in general relativity*, Phys. Rev. **D 85** (2012) 023504 [arXiv:1107.5427] [INSPIRE].

[16] N. Kaiser and M.J. Hudson, *On the perturbation of the luminosity distance by peculiar motions*, Mon. Not. Roy. Astron. Soc. **450** (2015) 883 [arXiv:1411.6339] [INSPIRE].

[17] SNLS collaboration, J.D. Neill, M.J. Hudson and A.J. Conley, *The peculiar velocities of local type Ia supernovae and their impact on cosmology*, Astrophys. J. **661** (2007) L123 [arXiv:0704.1654] [INSPIRE].

[18] SDSS collaboration, M. Betoule et al., *Improved cosmological constraints from a joint analysis of the SDSS-II and SNLS supernova samples*, Astron. Astrophys. **568** (2014) A22 [arXiv:1401.4064] [INSPIRE].

[19] SNLS collaboration, A. Conley et al., *Supernova constraints and systematic uncertainties from the first three years of the Supernova Legacy Survey*, Astrophys. J. Suppl. **192** (2011) 1 [arXiv:1104.1443] [INSPIRE].

[20] SDSS collaboration, M. Betoule et al., *Improved photometric calibration of the SNLS and the SDSS supernova surveys*, Astron. Astrophys. **552** (2013) A124 [arXiv:1212.4864] [INSPIRE].

[21] WMAP collaboration, G. Hinshaw et al., *Five-year Wilkinson Microwave Anisotropy Probe (WMAP) observations: data processing, sky maps and basic results*, Astrophys. J. Suppl. **180** (2009) 225 [arXiv:0803.0732] [INSPIRE].

[22] R. Amanullah et al., *Spectra and Hubble Space Telescope light curves of six type Ia supernovae at $0.511 < z < 1.12$ and the Union2 compilation*, Astrophys. J. **716** (2010) 712 [arXiv:1004.1711] [INSPIRE].

[23] N. Suzuki et al., *The Hubble Space Telescope Cluster Supernova Survey. V. Improving the dark-energy constraints above $z > 1$ and building an early-type-hosted supernova sample*, Astrophys. J. **746** (2012) 85 [arXiv:1105.3470] [INSPIRE].

[24] S. Jha, A.G. Riess and R.P. Kirshner, *Improved distances to type Ia supernovae with multicolor light-curve shapes: MLCS2k2*, Astrophys. J. **659** (2007) 122 [astro-ph/0612666] [INSPIRE].

[25] D.L. Shafer and D. Huterer, *Chasing the phantom: a closer look at type Ia supernovae and the dark energy equation of state*, Phys. Rev. **D 89** (2014) 063510 [arXiv:1312.1688] [INSPIRE].

[26] PLANCK collaboration, P.A.R. Ade et al., *Planck 2015 results. XIII. Cosmological parameters*, arXiv:1502.01589 [INSPIRE].

[27] I. Ben-Dayan, R. Durrer, G. Marozzi and D.J. Schwarz, *The value of H_0 in the inhomogeneous universe*, Phys. Rev. Lett. **112** (2014) 221301 [arXiv:1401.7973] [INSPIRE].

[28] C. Gordon, K. Land and A. Slosar, *Cosmological constraints from type Ia supernovae peculiar velocity measurements*, Phys. Rev. Lett. **99** (2007) 081301 [arXiv:0705.1718] [INSPIRE].

[29] A. Cooray, D. Holz and D. Huterer, *Cosmology from supernova magnification maps*, Astrophys. J. **637** (2006) L77 [astro-ph/0509579] [INSPIRE].

[30] S. Hannestad, T. Haugboelle and B. Thomsen, *Precision measurements of large scale structure with future type-IA supernova surveys*, JCAP **02** (2008) 022 [arXiv:0705.0979] [INSPIRE].

[31] A. Abate and O. Lahav, *The three faces of Ω_m: testing gravity with low- and high-redshift SN Ia surveys*, Mon. Not. Roy. Astron. Soc. **389** (2008) 47 [arXiv:0805.3160] [INSPIRE].

[32] S. Bhattacharya, A. Kosowsky, J.A. Newman and A.R. Zentner, *Galaxy peculiar velocities from large-scale supernova surveys as a dark energy probe*, Phys. Rev. **D 83** (2011) 043004 [arXiv:1008.2560] [INSPIRE].

[33] T. Castro and M. Quartin, *First measurement of σ_8 using supernova magnitudes only*, Mon. Not. Roy. Astron. Soc. **443** (2014) L6 [arXiv:1403.0293] [INSPIRE].

[34] Y.-Z. Ma, C. Gordon and H.A. Feldman, *The peculiar velocity field: constraining the tilt of the universe*, Phys. Rev. **D 83** (2011) 103002 [arXiv:1010.4276] [INSPIRE].

[35] R. Watkins, H.A. Feldman and M.J. Hudson, *Consistently large cosmic flows on scales of $100\,h^{-1}$Mpc: a challenge for the standard ΛCDM cosmology*, Mon. Not. Roy. Astron. Soc. **392** (2009) 743 [arXiv:0809.4041] [INSPIRE].

[36] J. Colin, R. Mohayaee, S. Sarkar and A. Shafieloo, *Probing the anisotropic local universe and beyond with SNe Ia data*, Mon. Not. Roy. Astron. Soc. **414** (2011) 264 [arXiv:1011.6292] [INSPIRE].

[37] D.-C. Dai, W.H. Kinney and D. Stojkovic, *Measuring the cosmological bulk flow using the peculiar velocities of supernovae*, JCAP **04** (2011) 015 [arXiv:1102.0800] [INSPIRE].

[38] S.J. Turnbull et al., *Cosmic flows in the nearby universe from type Ia supernovae*, Mon. Not. Roy. Astron. Soc. **420** (2012) 447 [arXiv:1111.0631] [INSPIRE].

[39] U. Feindt et al., *Measuring cosmic bulk flows with type Ia supernovae from the Nearby Supernova Factory*, Astron. Astrophys. **560** (2013) A90 [arXiv:1310.4184] [INSPIRE].

[40] G.J. Mathews, B. Rose, P. Garnavich, D. Yamazaki and T. Kajino, *Detectability of cosmic dark flow in the type-IA supernova redshift-distance relation*, arXiv:1412.1529 [INSPIRE].

[41] T. Haugboelle et al., *The velocity field of the local universe from measurements of type Ia supernovae*, Astrophys. J. **661** (2007) 650 [astro-ph/0612137] [INSPIRE].

[42] A. Weyant, M. Wood-Vasey, L. Wasserman and P. Freeman, *An unbiased method of modeling the local peculiar velocity field with type Ia supernovae*, Astrophys. J. **732** (2011) 65 [arXiv:1103.1603] [INSPIRE].

[43] Y.-Z. Ma and D. Scott, *Cosmic bulk flows on $50\,h^{-1}$Mpc scales: a Bayesian hyper-parameter method and multishell likelihood analysis*, Mon. Not. Roy. Astron. Soc. **428** (2013) 2017 [arXiv:1208.2028] [INSPIRE].

[44] A. Johnson et al., *The 6dF Galaxy Survey: cosmological constraints from the velocity power spectrum*, Mon. Not. Roy. Astron. Soc. **444** (2014) 3926 [arXiv:1404.3799] [INSPIRE].

[45] Y.-Z. Ma and J. Pan, *An estimation of local bulk flow with the maximum-likelihood method*, Mon. Not. Roy. Astron. Soc. **437** (2014) 1996 [arXiv:1311.6888] [INSPIRE].

[46] D.J. Schwarz and B. Weinhorst, *(An)isotropy of the Hubble diagram: comparing hemispheres*, *Astron. Astrophys.* **474** (2007) 717 [arXiv:0706.0165] [INSPIRE].

[47] B. Kalus, D.J. Schwarz, M. Seikel and A. Wiegand, *Constraints on anisotropic cosmic expansion from supernovae*, *Astron. Astrophys.* **553** (2013) A56 [arXiv:1212.3691] [INSPIRE].

[48] X. Yang, F.Y. Wang and Z. Chu, *Searching for a preferred direction with Union2.1 data*, *Mon. Not. Roy. Astron. Soc.* **437** (2014) 1840 [arXiv:1310.5211] [INSPIRE].

[49] S. Appleby, A. Shafieloo and A. Johnson, *Probing bulk flow with nearby SNe Ia data*, *Astrophys. J.* **801** (2015) 76 [arXiv:1410.5562] [INSPIRE].

[50] H.-N. Lin, S. Wang, Z. Chang and X. Li, *Testing the isotropy of the universe by using the JLA compilation of type-Ia supernovae*, arXiv:1504.03428 [INSPIRE].

[51] B. Javanmardi, C. Porciani, P. Kroupa and J. Pflamm-Altenburg, *Probing the isotropy of cosmic acceleration traced by type Ia supernovae*, *Astrophys. J.* **810** (2015) 47 [arXiv:1507.07560] [INSPIRE].